

**INTERNATIONAL JOURNAL OF ENGINEERING SCIENCES & RESEARCH  
TECHNOLOGY****A REVIEW ON CORROSION BEHAVIOUR OF SHAPEMEMORY ALLOYS.****A G Shivasiddaramiah<sup>1</sup>, U S Mallik<sup>2</sup>, Ranjit Mahato<sup>3</sup>, C Shashishekar<sup>4</sup> & Prashantha S.<sup>5</sup>**<sup>\*1&5</sup> Assistant Professor, Department of Mechanical Engineering, Siddaganga Institute of Technology, Tumakuru-572-103, Karnataka, India.<sup>2</sup> Professor, Department of Mechanical Engineering, Siddaganga Institute of Technology, Tumakuru-572-103, Karnataka, India.<sup>3</sup> U G Scholar, Department of Mechanical Engineering, Siddaganga Institute of Technology, Tumakuru-572-103, Karnataka, India.<sup>4</sup> Associate Professor, Department of Mechanical Engineering, Siddaganga Institute of Technology, Tumakuru-572-103, Karnataka, India.**ABSTRACT**

Shape memory alloys after deformation achieve its geometry by itself on heating or at an elevated temperature simply on unloading (super elasticity or pseudo elasticity) added with excellent bending and corrosion resistance, magnetic and biological resonance capability, illustrate the wide application of shape memory alloys in the manufacturing of biomedical devices in last 20 years. A detail review has been made in the corrosive behavior of Cu-based SMAs with different microstructures. This Cu-based SMAs namely Cu-Al, Cu-Zn-Al, Cu-Zn-Ni, Cu-Al-Be, Cu-Al-Be-Mn, at high temperature demonstrate  $\beta$ -phase and reveals shape memory effect thereafter quenching under low temperatures thus processed by ingot metallurgy. Bending test conforms the shape memory effect. Alloy microstructure highly affects the corrosion behavior and  $\beta$ -samples present higher pitting resistance and repassivation capability.

**KEYWORDS:** shape memory effect, corrosion, corrosion behavior, Hank's Solution.**INTRODUCTION**

Alloys exhibiting the shape memory effect can withstand numerous huge amount of strain and then, regain its initial shape upon elevated temperature or strain unloading [1]. Namely shape memory alloys are categorized into two broad classes: ferrous alloys and the other one is non-ferrous alloys. The ferrous SMA consists of 'Fe', 'Mn', and 'Si' as major alloying elements. The costs of the ferrous SMAs are less than non-ferrous alloys. But the shape memory effect exhibited by these alloys are one way, further, certain limitations are shown by these alloys on shape memory effect itself. Therefore, a need arises to investigate other alloys for SMAs [2]. The corrosive characters shown by Cu-based alloys, e.g. Cu-Al, Cu-Zn-Al, Cu-Zn-Ni, Cu-Al-Be, Cu-Al-Be-Mn, has been inquired since many decades. Belkahl et al. [3] brought into light that mixing of a limited amount of beryllium in Cu-Al based arrangement can effectively depress the martensitic alteration temperatures without altering the stability of high temperature  $\beta$ -phase. In investigation it is concluded beryllium can reorganize mechanical behavior and microstructure of SMAs. Up to now, its unclear what's the role of beryllium on corrosion character of Cu-Al based SMAs. It was found that mixing of aluminum to Cu-based alloys increases the corrosion resistivity if the alloys are disclosed to high temperature environments or atmosphere consisting of sulfide [4]. Also, Sylwestrowicz [5] brought into light that grain boundaries of Cu-Be alloys were like to be attacked at the initial phase among the two-phases related to stress corrosion. Data on the corrosive nature of Cu-Al based shape memory alloys (SMAs), particularly Cu-Al-Be SMAs, are very less. Cu-based SMAs are commonly are of Cu-Al system, in martensitic transformation temperature decreasing elements like Cu-Zn-Al, Cu-Al-Ni, Cu-Al-Mn, and Cu-Al-Be are added. The quaternary Cu-Al-Be-Mn alloy has distinct mechanical peculiarity such like exceptional shape recognition capability, high mechanical strength, strong damping capability due to the martensitic transformation and pseudoelastic, distinctive ability to take in vibrations, sound and mechanical waves because of coarse grain size provide higher resistance to corrosion, minimum manufacturing cost, good utility at lesser temperatures compared to Ni-Ti Alloy which is costly [6]. Due to functional abilities of these alloys, the uses of SMAs have been extraordinarily fruitful in biomedical aspects, enhance both the performance and possibility of minimally invasive surgeries. The main specialty to its

[ICAMS-2017: March, 17]

IC<sup>TM</sup> Value: 3.00

application for biomedical is its biocompatibility[7]. Due to their good biocompatibility, another important field of SMA application is medical science, the pseudo-elasticity is frequently used for the recognition of different components such as micro surgical and endoscopic devices, cardiovascular stent, orthopedic components, embolic protection filters, and orthodontic wires[ 8].

## GENERAL METHODOLOGY

### Alloy Preparation Procedure

Cu-based SMAs were chosen containing the exact amount of Al, Be, Mn, Zn or Ni and rest copper. A right amount of combination was taken to weight 200grams of alloy for melting in induction furnace in an inert argon environment.

Then hot, molten metal alloy was drained in a pre-heated cast iron mould of dimension of 120mm X 100mm X 3mm and allows solidifying. The ingot was further homogenized at nearly about 900°C in  $\beta$ -phase for nearly about 4-6 hours in argon atmosphere which was further hot rolled in 800°C to the thickness of 1mm. For 30minutes at 800°C, the samples were re-homogenized and up on a hot water bath of 100°C, it was step quenched which is pursued by quenching in room temperature water bath i.e. 25°C. It was done to eradicate quench cracks as well as binding of martensites by surplus quenched in vacancies maintain on quenching from a high temperature. The study of microstructure was done by the help of Optical Microscope [9].

### Preparation of Substitute Ocean Water

As per ASTM D 1141-98(Reapproved, 2003) substitute Ocean water was prepared from two stock solutions. These standard solutions were prepared as shown in the table below and blended in right proportion to make 10L of Ocean water [9]

*Table1 (a).Standard solution No. 1 composition (g/L)*

MgCl <sub>2</sub> .6H <sub>2</sub> O	3889.00g(=555.60g/L)
CaCl <sub>2</sub> (fused)	405.60g(=57.90g/L)
SrCl <sub>2</sub> .6H <sub>2</sub> O	14.80g(=2.10g/L)

*Table1 (b).Standard solution No. 2 composition (g/L)*

KCl	486.20g(=69.50g/L)
NaHCO <sub>3</sub>	140.70g(=20.10g/L)
KBr	70.40g(=10.00g/L)
H <sub>3</sub> BO <sub>3</sub>	19.00g(=2.70g/L)
NaF	2.10g(0.30g/L)

10L of Ocean water was prepared by adding 254.35 grams of sodium chloride and 40.49 grams of anhydrous sodium sulphate in 8 to 9 Liters of distil water. Again 200 ml of Standard Solution No. 1 was poured and was stirred thoroughly followed by mixing 100 ml of Standard Solution No. 2. The prepared solution was diluted to 10L and the pH was attuned to 8.2 with small amount of 0.1N sodium hydroxide solutions [9].

### Preparation of Hank's Solution

NaCl	8.00g/L
Glucose	1.00g/L
KCl	0.40g/L
MgCl <sub>2</sub> .6H <sub>2</sub> O	0.10g/L
Na <sub>2</sub> HPO <sub>4</sub> .2H <sub>2</sub> O	0.06g/L
KH <sub>2</sub> PO <sub>4</sub>	0.06g/L
MgSO <sub>4</sub> .7H <sub>2</sub> O	0.06g/L
CaCl <sub>2</sub>	0.14g/L
NaHCO <sub>3</sub>	0.35g/L

[ICAMS-2017: March, 17]

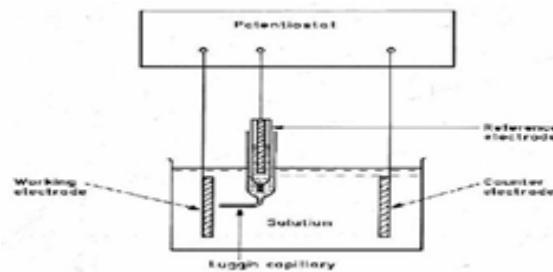
IC<sup>TM</sup> Value: 3.00

The above salts were made to dissolve in 1L of distilled water. At the temperature of 37°C, 7.2 pH was maintained (Zheng et al., 2006).

### Corrosion Test Procedure

A flat square piece of size 20mmX20mmX1mm was cut from the prepared shape memory alloy and polished with emery papers of different sizes and then with Al<sub>2</sub>O<sub>3</sub> powder. The microstructure was studied for the polished sample and then the specimen was subjected to mainly three different corrosive mediums i.e. fresh water, ocean water and Hank's solution. 150ml of above prepared solution was used for standard test cell. The area of 0.16cm<sup>2</sup> was exposed to the electrolyte solution after placing the samples and electrodes in the respective places. As reference electrode, standard calomel electrode, was kept in respective holder and joined to the potentiostat. With the help of the software called Princeton Applied Research 352 Softcorr<sup>TM</sup> III corrosion measurement, the voltage and current values were obtained in the pattern of E-I plot. The corrosion potentials  $E_{corr}$ ,  $E_{pit}$  and microstructure of the sample after corrosion were studied and recorded [9].

(a)



(b)

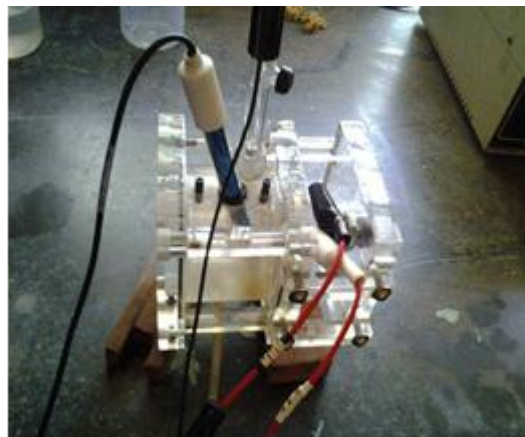


Figure :(a) electrochemical cell schematic figure, and (b) set up of electrochemical testing.

## RESULTS AND DISCUSSION

### Chemical Compositions

The chemical composition of the specimen was found out using of Perkin-Elmer inductively coupled plasma-optical emission spectrophotometer (ICP-OES).

*Table2 (a): chemical composition of Cu-Al-Be-Mn Shape Memory Alloys[9].*

Alloy Tag	Chemical Composition in Weight%			
	Cu	Al	Be	Mn
CABM1	87.89	11.5	0.41	0.20
CABM2	86.81	12.5	0.44	0.25
CABM3	87.25	12.0	0.45	0.30
CABM4	88.63	10.5	0.52	0.35

*Table2 (b): chemical composition of Cu-Al-BeShape Memory Alloys [10].*

Alloy Tag	Chemical composition in Weight%		
	Cu	Al	Be
CAB1	88.60	11.0	0.4
CAB2	88.49	11.1	0.41
CAB3	88.38	11.2	0.42
CAB4	88.27	11.3	0.43

*Table2 (c): chemical composition of Cu-Zi-Nishape memory alloys [11].*

Alloy Tag	Chemical composition in Weight %		
	Cu	Ni	Zn
CZN1	48.22	45.00	6.65
CZN2	48.96	48.04	2.96
CZN3	39.14	51.09	9.61
CZN4	50.49	44.93	3.05

### Microstructure

The properties like mechanical and physical properties are highly influenced by the microstructure which in turn determines the uses of these materials. Although the alloys show the parent austenitic stage in the cast situation, after step quenching transforms absolutely to lath type of martensite, showing the fully changeover of austenite into martensite without formation of precipitate[10].From the micro structural perspective, shape memory and pseudo-elastic effects are the result of reversible solid state micro structural transition from austenite to martensite, that can be stimulated by mechanical and/or thermal loads [12].The specimen for microstructure analysis were prepared by the standard metallographic method.

The microstructure is determined by the composition of the alloys. Different composition has different microstructure. Figures show the different in microstructure due to composition and percentage weight.

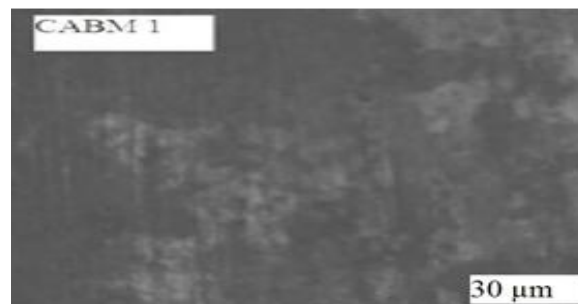


*Figure: CABM 1 after corrosion in fresh water [9]*

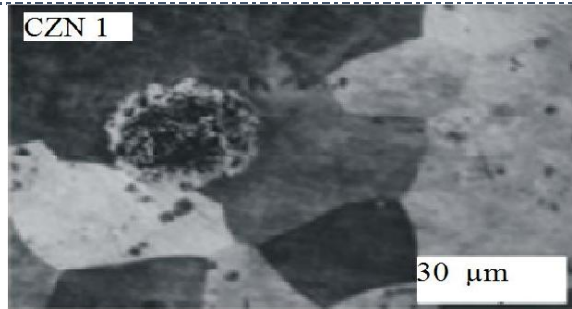


*Figure: CZN 1 after corrosion in fresh water [11]*

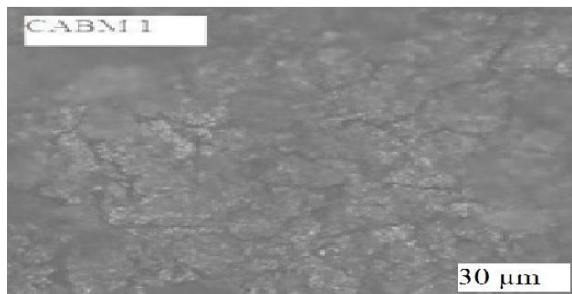


*Figure: CABM 1 after corrosion in Ocean Water [9]*

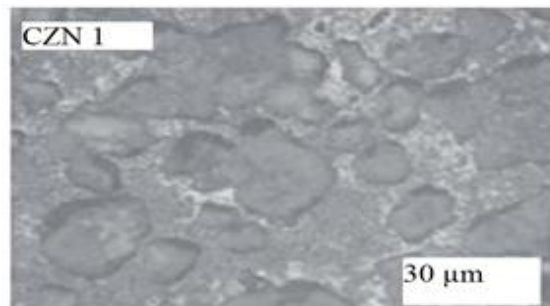


*Figure: CZN 1 after corrosion in Ocean Water [11]*

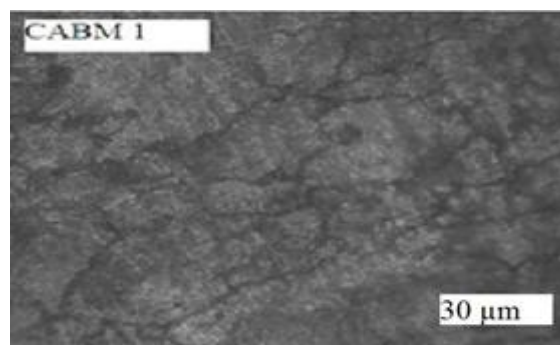


*Figure: CABM 1 after corrosion in Hank's solution [9].*

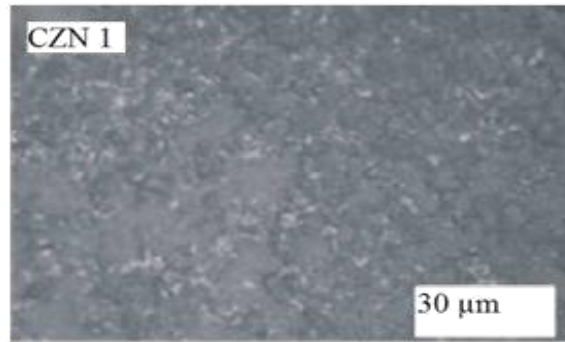


Figure: CZN 1 after corrosion in Hank's solution [11]

### SHAPE MEMORY EFFECT

The Shape memory effect of the alloys was determined by using Bend test [10].  
The formula to calculate the shape memory effect is given as

$$\% \text{ S.M.E} = \theta_m / (180 - \theta_e).$$

The figure below explains the bend test.

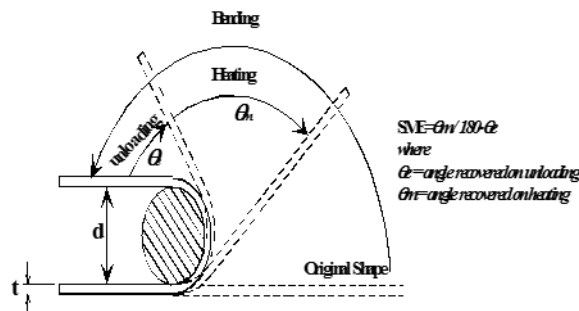


Figure: Schematic figure of the bend test to determine strain recovery by SME. [9]

Table3 (a): Shape Memory Effect of Cu-Al-Be-Mn Shape Memory Alloys [9].

Alloy Tag	Thickness (t) mm	Dia (d) mm	$\theta_m$	$\theta_c$	S.M.E %
CABM1	1	32	117	38	82.39
CABM2	1	32	117.6	40	84
CABM3	1	32	127	33	86.39
CABM4	1	32	115.5	56	93.10

Table3 (b): Shape Memory Effect of Cu-Al-Be Shape Memory Alloy [10].

CAB9	1	32	60	2	66
CAB10	1	32	72	2.5	80
CAB11	1	32	78	3	87
CAB12	1	32	80	3.5	89

Table3 (c): Shape Memory Effect of Cu-Zn-Ni Shape Memory Alloy [11].

Alloy Id	SME%
CZN1	66
CZN2	60
CZN3	72
CZN4	68

### Corrosion rate and Corrosion Potentials

The corrosion rate and corrosion potential was determined by using Metallurgical was determined by using Metallurgical Corrosion Analyzer System Gill AC and Electrochemical Corrosion Cell. A table containing



corrosion rate,  $I_{corr}$ ,  $E_{corr}$  and  $E_{pit}$  for fresh water, ocean water solution and Hank's solution is given below. The point where depletion of passive layer initiates on surface of material is  $E_{corr}$  and the complete depletion and initiations of pits is given by  $E_{pit}$ . From table, it was observed that there is no pit formation (Epit) in fresh water. It was also observed that the values of corrosion rate,  $I_{corr}$ ,  $E_{corr}$  and  $E_{pit}$  are higher in case of ocean water solution than in Hank's solution. From the result obtained, it can be concluded that with increase in %wt. of beryllium corrosion resistance increases [9].

**Table4 (a): Corrosion rate,  $E_{corr}$  and  $I_{corr}$  values of CABM [9]**

Alloy Id	In fresh Water			In Ocean Water				In Hank's Solution			
	Corrosion Rate (mm/yr)	$I_{corr}$ (MA/cm <sup>2</sup> )	$E_{corr}$ (mv)	Corrosion Rate (mm/yr)	$I_{corr}$ (MA/cm <sup>2</sup> )	$E_{corr}$ (mv)	$E_{pit}$ (mv)	Corrosion Rate (mm/yr)	$I_{corr}$ (MA/cm <sup>2</sup> )	$E_{corr}$ (mv)	$E_{pit}$ (mv)
CA 1	0.04198	0.00231	-	4.7455	0.2620	-	250.0	3.1771	0.1203	-	40.0
BM 2	0.01968	0.00111	-20.98	4.4618	0.2520	-	-10.0	2.9832	0.1685	-	85.0
CA 3	0.01850	0.00103	13.10	3.8491	0.2146	-	-25.0	2.4962	0.1392	-	55.0
BM 4	0.01550	0.00100	-	3.2699	0.2051	-	-5.0	2.3551	0.1274	-	50.0

**Table4 (b):  $E_{corr}$  and  $I_{corr}$  values of CZN [11].**

Alloy ID	In Fresh Water		In Ocean Water		In Hank's Solution	
	$E_{corr}$ (mv)	$E_{pit}$ (mv)	$E_{corr}$ (mv)	$E_{pit}$ (mv)	$E_{corr}$ (mv)	$E_{pit}$ (mv)
CZ N1	-73.847	-	-254.88	470.31	-184.26	664.41
CZ N2	-99.3	823.78	-273.14	414.73	-208.98	589.04
CZ N3	-24.64	911.30	-333.79	413.15	-164.49	833.27
CZ N4	-80.99	850.54	-252.8	313.78	201.58	486.25

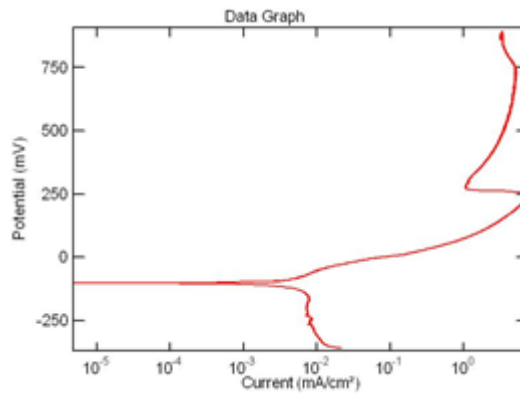


Figure :(a) Potentiodynamic curve of CABM1 in artificial ocean water [9].

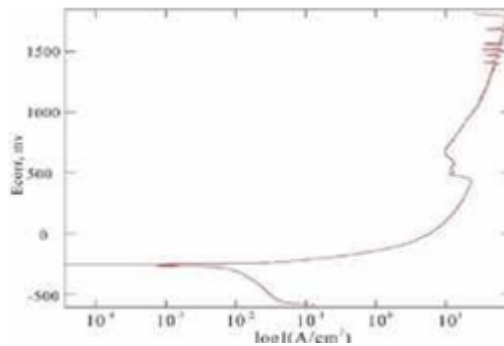


Figure :(b) Potentiodynamic curve of CZN1 in artificial ocean water [11].

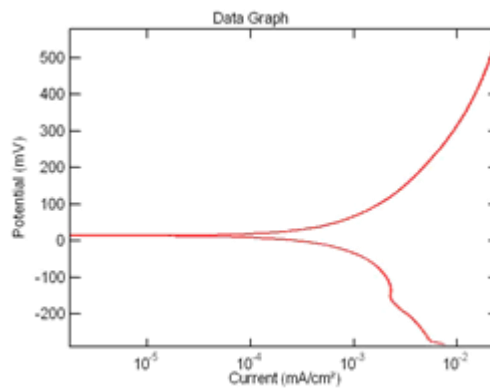


Figure :(c) Potentiodynamic curve of CABM 3 in fresh water[9].

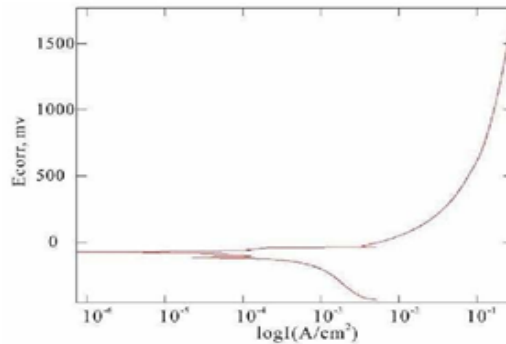


Figure :(d) Potentiodynamic curve of CZN 1 in fresh water [11].



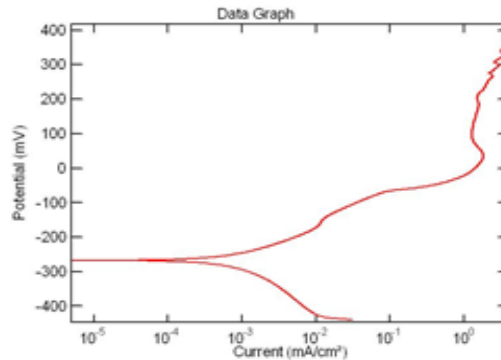


Figure (e) Potentiodynamic curve of CABM 1 in Hank's solution [9].

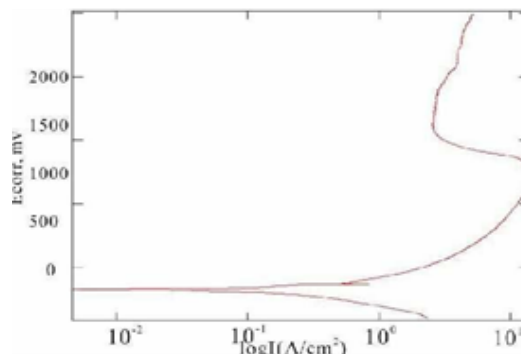


Figure (f) Potentiodynamic curve of CZN 3 in Hank's solution [11].

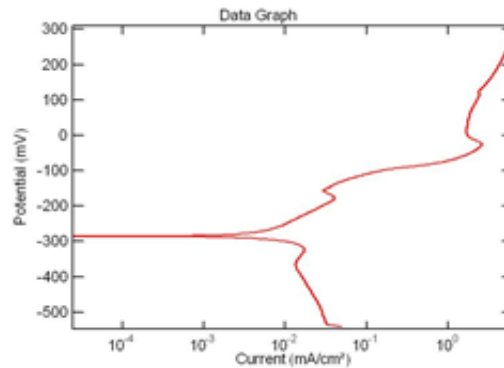


Figure (g) Potentiodynamic curve of CABM 3 in artificial sea water [10].

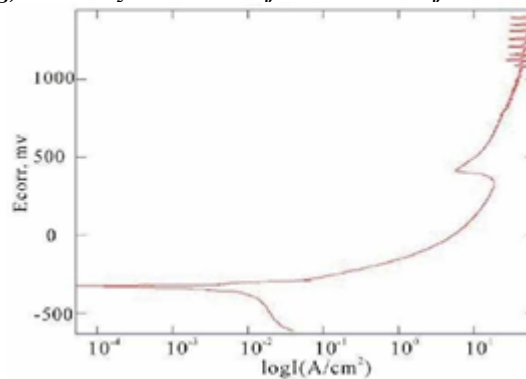


Figure (h) Potentiodynamic curve of CZN 3 in artificial Ocean water [11].

---

**DISCUSSION****Effect of Al in corrosion behavior of Cu-based SMAs.**

The corrosion behavior of copper decrease with the increase in concentration of aluminum. Although there is increase in corrosion resistance in Cu-Al alloys with increase in aluminum concentration, the intergranular corrosion occurs [4].

**Effect of Zn in corrosion behavior of Cu-based SMAs.**

It was seen that customizing in structure due to phase transformation affected the corrosive nature of Cu-Zn-Al shape memory alloys. The corrosion resistance increase with the increasing concentration of Zinc. Cu-Zn-Al shape memory alloy forms intermetallic compound of  $\gamma\text{Cu}_5\text{Zn}_8$  in sintering state, also it forms  $\beta\text{Cu}_{0.61}\text{Zn}_{0.39}$  in quenching state [14].

**Effect of Ni in corrosion behavior of Cu-based SMAs.**

With the increase wt% of Ni content in Cu-Zn-Ni SMAs the corrosion resistance of the alloy also increases in the corrosive medium. It was found out that these alloys shows excellent corrosion resistance in fresh water in comparison to sea water and Hank's solution [14]. Because of better thermal stability and operating temperature is high, Cu-Al-Ni is better choice than Cu-Zn-Al for practical high-temperature shape-memory alloys [15]. Ni shows pitting corrosion in Hank's solution [11].

**Effect of Be in corrosion behavior of Cu-based SMAs.**

Addition of beryllium shows valuable effect in Cu-based SMAs [16]. Kuo et al. found that small amount of beryllium, between 0.55 to 1.00 wt. %, in Cu-Al-Be alloys are sufficient in prevent the intergranular corrosion [4] as well as just 0.1% of beryllium decreases the phase transformation temperature of alloys by approx. 100°C[17]. Beryllium atoms in the polycrystalline Cu-Al-Be SMAs are supposed to be able to diffuse into grain boundary in which beryllium atoms diffuse byvacancy mechanism during quenching. This deactivates grain boundaries and avoids the intergranular corrosion of Cu-Al SMAs. Also, SMAs with same beryllium contains and different microstructure has different corrosion rates.

**Effect of Mn in corrosion behavior of Cu-based SMAs.**

Addition of Manganese reduces the brittleness and increases the ductility of the alloy [12, 18].By increasing in wt.% of manganese in an alloy, there is an increase in Ultimate Tensile Strength linearly and decrease in corrosion rate[9,18]. It was seen that Cu-Al-Be-Mn SMA's show good Shape Memory Effect up to 95.1 % and alternation in chemical composition effects the Shape Memory Effect [6].

**CONCLUSION**

- a) Copper-based SMAs have some advantages over other SMAs such as low cost and easy to synthesise; thorough study is being made on these SMAs [12].
- b) Copper-based shape-memory alloys are oversensitive to thermal effects, and it is possible that in thermal cycles its properties change (e.g., shape-recovery ratio, transformation temperatures, and crystal structures, hysteresis and mechanical behavior) [19].
- c) The quaternary addition in an alloy is best known for the Shape Memory properties, the ternary addition is best known for its higher transition temperature [20].
- d) Corrosion rate for alloys has been decreased with increasing the percent of alloying elements (Mn, Ti) [14].
- e) The main aim for the study of Cu-Al-Be-Mn shape memory alloys is due to their benefit over ternary shape memory alloy, which suffers from brittleness at the working (low) temperature [12].
- f) The corrosion rate of the Cu-Al-Be-Mn is less in fresh water as compared to Hank's solution and ocean water [9].
- g) Cu-Al-Be-Mn SMA's exhibit good corrosion resistance Ecorr value of -20.98 in fresh water, -282.11 in hank's solution and -294.19 in ocean water were observed in these alloys [9]

- h) The wide use of SMAs in biomedical field is due to their functional qualities, strengthening possibility and the execution of less invasive surgeries [7].
- i) Ni-release may cause allergic reactions in an organism and there is pitting occurring in the alloy samples in Hanks solution, it cannot be a promising alternative for biomedical application. So studies are made to replace NiTi SMAs with ternary SMAs in biomedical field [11, 21].
- j) The corrosion behavior is strongly affected by the alloy microstructures conditions, and the samples with single  $\beta$ -phase present a better behavior: higher pitting resistance and repassivationability [16].
- k) The MS temperature decreases with aluminum and beryllium compositions [10].

## REFERENCES

- [1] Vanja Asanović and Kemal Deljić, "The Mechanical Behavior and Shape Memory Recovery of Cu-Zn-Al Alloys", Association of Metallurgical Engineers of Serbia Review paper AMES UDC: 669.35'571.018.2:620.172.7=20
- [2] S Balasubramani, Dr.T.Vigraman "Effect of Cu and Ni addition in Fe-Mn-Si shape memory alloy" International Journal of Scientific & Engineering Research, Volume 5, Issue 5, May-2014 183 ISSN 2229-5518
- [3] S. Belkahla, H. Flores Zuniga, G. Guenin, Mater. Sci. Eng.: A 169 (1993) 119–124.
- [4] H.H. Kuo, W.H. Wang, Y.F. Hsu, C.A. Huang, "The corrosion behavior of Cu–Al and Cu–Al–Be shape-memory alloys in 0.5 M H<sub>2</sub>SO<sub>4</sub> solution", Corrosion Science 48 (2006) 4352-4364
- [5] W.D. Sylwestrowicz, Corrosion 25 (10) (1969) 405–415.
- [6] Shivasiddaramaiah.A.G, Manjunath.S.Y, Prashant Singh, U.S.Mallikarjun "Synthesis and Evaluation of Mechanical Properties of Cu-Al-Be-Mn Quaternary Shape Memory Alloys"
- [7] L.G. Machado and M.A. Savi, Medical applications of shape memory alloys, Brazilian Journal of Medical and Biological Research (2003) 36: 683-691, ISSN 0100-879X Review
- [8] B. Chen, C. Liang, D. Fu, Pitting Corrosion of Cu-Zn-Al Shape Memory Alloy in Simulated Uterine Fluid, J. Mater. Sci. Technology, 21(2) (2005) 226-230.
- [9] Shivasiddaramaiah.A.G, Ravi Das B.R.D, Prashant Singh, U.S.Mallikarjun, "Study on Corrosion Behaviour of Cu-Al-Be-Mn Quaternary Shape Memory Alloy At Room Temperature", International Journal of Applied Engineering Research, ISSN 0973-4562 Vol.10 No.55 (2015) © Research India
- [10] Ranganatha Swamy MK, Prashantha S, U.S.Mallikarjun, "Characterization of Cu-Al-Be Shape Memory Alloys", IOSR Journal of Mechanical and Civil Engineering (IOSR-JMCE) ISSN: 2278-1684, PP: 01-06
- [11] S. Sathish, U. S. Mallik, T. N. Raju, "Corrosion Behavior of Cu-Zn-Ni Shape Memory Alloys", Journal of Minerals and Materials Characterization and Engineering, 2013, 1, 49-54 <http://dx.doi.org/10.4236/jmmce.2013.12010> Published Online March 2013 (June 2014)
- [12] Shivasiddaramaiah.A.G, Prashant Singh, Manjunath S.Y, U.S.Mallikarjun, "Microstructure and Shape Memory Effect of Cu-Al-Be-Mn Quaternary Shape Memory Alloys", Applied Mechanics and Materials Vols. 813-814 (2015) pp 213-217 Submitted: 2015-04-23 © (2015) Trans Tech Publications, Switzerland Revised: 2015-06-11 Accepted: 2015-07-12
- [13] Y. Liu, G.S. Tan, Formation of interfacial voids in cast and micro-grained  $\gamma'$ -Ni<sub>3</sub>Al during high temperature oxidation, Intermetallics (2000) 8 1385-1391
- [14] Jassim Mohammed Salman A, Abdul Raheem K. Abid Ali A and Huda Abbas Kheralla A "Corrosion study of CuAlZn Shape Memory Alloys in 3.5 NaCl Solution", Materials Engineering College, Babylon University, Iraq, Accepted 30 May 2014, Available online 01 June 2014, Vol.4, No.3 (June 2014)
- [15] Z. G. WEI, R. SANDSTROM, S. MIYAZAKI "Review Shape-memory materials and hybrid composites for smart systems, Part I Shape memory materials", JOURNAL OF MATERIALS SCIENCE 33 (1998) 3743-3762
- [16] S. Montecinos, S. Simisonb, "Corrosion behavior of Cu–Al–Be shape memory alloys with different compositions and microstructures", Corrosion Science 74 (2013) 387–395
- [17] S. Belkahla, H.F. Zuñiga, G. Guenin, Elaboration and characterization of new low temperature shape memory Cu–Al–Be alloys, Materials Science and Engineering: A, 169, 1993, p 119-124.
- [18] Shivasiddaramaiah.A.G, Manjunath.S.Y, Prashant Singh, U.S.Mallikarjun, "Synthesis and Evaluation of Mechanical Properties of Cu-Al-Be-Mn Quaternary Shape Memory Alloys",
- [19] Vittorio Di Cocco, Francesco Iacoviello, Luigi Tomassi, Stefano Natali, Valerio Volpe, "Crack initiation and growth in an Zn-Cu-Al PE alloy", 13th International Conference on Fracture June 16–21, 2013, Beijing, China

---

[20]RupaDasgupta , Ashish Kumar Jain, Pravir Kumar, Shahadat Hussein, Abhishek Pandey, “Effect of alloying constituents on the martensitic phase formation in some Cu-basedSMAs”, CSIR-Advanced Materials and Processes Research Institute (AMPRI), Bhopal, India

[21]Nader El-Bagoury, Mohammed A. Amin<sup>1</sup>,H. Shokry “Microstructure and Corrosion Behavior of Ni<sub>52</sub>Ti<sub>48-x</sub>Cox Shape Memory Alloys in 1.0 M HClSolution”,Nader El-Bagoury<sup>1,2\*</sup> , Mohammed A. Amin<sup>1,3</sup>, H. Shokry<sup>4,5</sup>Int. J. Electrochem. Sci., 8 (2013) 1246 – 1261